



## Original article

A novel *p*-terphenyl derivative inducing cell-cycle arrest and apoptosis in MDA-MB-435 cells through topoisomerase inhibitionJin Qiu<sup>a,b</sup>, Baobing Zhao<sup>a</sup>, Yan Shen<sup>a</sup>, Wang Chen<sup>a</sup>, Yudao Ma<sup>c,\*</sup>, Yuemao Shen<sup>a,\*\*</sup><sup>a</sup>Key Laboratory of Chemical Biology (Ministry of Education), School of Pharmaceutical Sciences, Shandong University, Jinan 250012, Shandong, PR China<sup>b</sup>School of Pharmaceutical Sciences, Shandong University of Traditional Chinese Medicine, Jinan 250355, Shandong, PR China<sup>c</sup>School of Chemistry and Chemical Engineering, Shandong University, Shanda South Road No. 27, Jinan 250100, PR China

## ARTICLE INFO

## Article history:

Received 13 January 2013

Received in revised form

15 July 2013

Accepted 18 July 2013

Available online 11 August 2013

## Keywords:

Terphenyls

Topoisomerase

Suppressors

Apoptosis

## ABSTRACT

A novel series of *p*-terphenyl derivatives (**1–4**, **1a–4a**) was successfully synthesized and their *in vitro* anticancer activities were evaluated. Compound **1**, showing the best antiproliferative activity with  $IC_{50} < 1 \mu M$  against MDA-MB-435 cells, was further investigated. Compound **1** brought about a remarkable accumulation of MDA-MB-435 cells in G2/M phase prior to the induction of apoptosis. Further antitumor mechanism study indicated that compound **1**, which inhibited the enzyme activity of Topo I and Topo II $\alpha$  by interfering predominantly with the enzyme, could be topoisomerase suppressors instead of poisons. We conclude that compound **1** represents a novel class of Topo catalytic suppressors for developing new chemotherapeutic agents.

© 2013 Elsevier Masson SAS. All rights reserved.

## 1. Introduction

Topoisomerases (Topo) are the essential enzymes that control and modify the topological state of DNA during cellular processes, such as replication, transcription, recombination, and chromatin remodeling [1,2]. Under normal conditions, the covalent Topo I or Topo II cleaved DNA intermediates are constitutively transient and, since the DNA relegation step is much faster than the cleavage one, they are tolerated by the cell. On the contrary, conditions that significantly alter the physiological concentration or the life time of these breaks play a crucial role in inhibiting cell cycle progression and cell death [3,4]. In this regard, they are now viewed as important therapeutic targets for cancer chemotherapy [5].

*p*-Terphenyl-type chemical entities, mainly found in mycomycetes, include scaffolds with a C-18 tricyclic or polycyclic C-18 skeleton which exhibiting alkylated side chains [6]. Members of this family of natural products, isolated from *A. candidus*, have displayed various degrees of cytotoxicity [7]. In our previous study, *p*-terphenyl derivatives, isolated from the marine fungal strain *Aspergillus* sp. AF119, were found showing potent cytotoxicity

against human hepatocellular carcinoma HepG2 cell line, human cervical carcinoma HeLa cell line and human breast carcinoma MDA-MB-435 cell line through the generation of ROS, cell cycle arrest and apoptosis [8]. Nevertheless, the detailed mechanism responsible for the anti-tumor activity has not been well elucidated. In order to uncover the basic pharmacophore of *p*-terphenyls and discover novel derivatives as potential anti-cancer agents, eight new *p*-terphenyl derivatives were successfully synthesized. Herein, preliminary structure–activity relationship (SAR) of derivatives for their *in vitro* cytotoxicity and antitumor mechanism of the compounds were discussed. Our results indicated that compound **1**, with its inhibition of the Topo I and Topo II $\alpha$  activities, could induce apoptosis and cell cycle arrest.

## 2. Results

## 2.1. Chemistry

The compounds **1–4** and **1a–4a** (Fig. 1A) were obtained via two different parallel synthetic methods based on palladium (0)-catalyzed aryl–aryl coupling reactions (Scheme 1). As shown in Scheme 1, the compounds were prepared from 4-hydroxyphenyl boronic acid (**7**) or 4-methoxyphenylboronic acid (**11**) via sequential Suzuki cross-coupling reactions. Bromide **5** was purchased from Aldrich and bromide **6** was prepared from

\* Corresponding author. Tel.: +86 531 88361869; fax: +86 531 88565211.

\*\* Corresponding author. Tel.: +86 531 88382108.

E-mail addresses: [ydma@sdu.edu.cn](mailto:ydma@sdu.edu.cn) (Y. Ma), [yshen@sdu.edu.cn](mailto:yshen@sdu.edu.cn), [ahua0966@sdu.edu.cn](mailto:ahua0966@sdu.edu.cn) (Y. Shen).

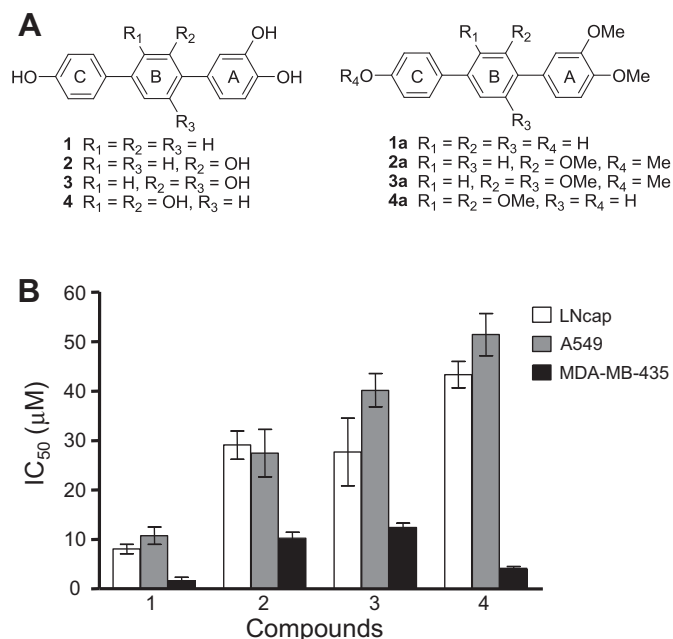


**Fig. 1.** *p*-Terphenyl derivatives inhibit cancer cells growth. (A) Structure of *p*-terphenyl derivatives; (B) Cytotoxicity evaluation of the compounds **1–4** against LNCap, A549 and MDA-MB-435 cells. The cytotoxicity of compounds was expressed as  $IC_{50}$ , which was defined as the concentration of compound that resulted in a 50% inhibition of growth rate. Each value represents the mean  $\pm$  SD of three independent experiments.

cyclohexanone according to the literature procedure described below. A cross-coupling Suzuki reaction between compound **5** (compound **6**) and compound **7** produced the corresponding biphenyl derivatives, which underwent Suzuki cross-coupling reaction with the boronic acid **9** to give intermediate compounds **1a** and **4a**.

Bromide **10a** and bromide **10b** were prepared from the commercially available 2-methoxyphenol and 2,6-dimethoxyphenol according to the literature described below. A cross-coupling Suzuki reaction between compound **10a** (compound **10b**) and compound **11** afforded the corresponding biphenyl derivatives, which reacted with trifluoromethanesulfonic anhydride and then with compound **9** via Suzuki reaction to give intermediate compounds **2a** and **3a**.

Finally, the parallel demethylation of compounds **1a**, **2a**, **3a** and **4a** with  $BBr_3$  at  $-78^\circ C$  produced the compounds **1**, **2**, **3** and **4**.

## 2.2. Biological studies

### 2.2.1. In vitro cytotoxicity of synthetic *p*-terphenyl derivatives against cancer cell lines

Compounds **1–4** showed evident anticancer effects against human prostate cancer cell line LNCap, human lung cancer cell line A549 and human breast carcinoma cell line MDA-MB-435 by the MTT assay (Fig. 1B). Compared with the other two ones, MDA-MB-435 cell line was more sensitive to compounds **1–4**. And the hydroxylation of benzene ring B of compounds **1–4** such as **2**, **3** and **4** decreased the cytotoxic activity against MDA-MB-435 cells. Similar to compound **3a**, compound **2a** was found to be inactive up to  $100 \mu M$ . These data indicated that the phenolic hydroxyl groups on the benzene ring A and C could be crucial to the cytotoxicity. Compound **1**, which exhibited the best activity against MDA-MB-435 cells with  $IC_{50} < 1 \mu M$ , was picked out for further studies.

### 2.2.2. Compound **1** induced cell-cycle arrest and apoptosis

Cell cycle arrest is an important sign for inhibition of proliferation. Flow cytometric analysis was applied to analyze the effect on the cell cycle after being treated with compound **1** for 24 h (Fig. 2A). After were treated with increasing concentration of compound **1**, the cell number of the cells at the G2/M phase increased significantly, while a corresponding decrease of that in the G1 and S phase. Meanwhile, a slight increase of cell number in the sub-G1 phase was observed after treatment with  $1 \mu M$  compound **1**. Besides accumulation of cells at the sub-G1 phase was in a time-dependent manner (Fig. 2D). All these results showed that compound **1** could induce a G2/M phase arrest and subsequent cell death.

Cell cycle arrest at G2/M phase is a common cellular response to a variety of DNA-damaging agents [9,10]. Therefore we next investigated whether the anti-tumor activity of compound **1** resulted from DNA damage response activation. DNA damage in cells evoked a checkpoint response which moderated cell cycle progression for repair of the damage. The molecular response to DNA damage began with the recognition of the DSBs followed by the activation of phosphatidylinositol 3-kinase-like kinase (PI3K) family members which were responsible for the phosphorylation of H2AX, such as ATM, ATR (ATM- and Rad3-related), and DNA-PK. Furthermore, p53 was stabilized and rapidly activated in response to DNA damage [11].

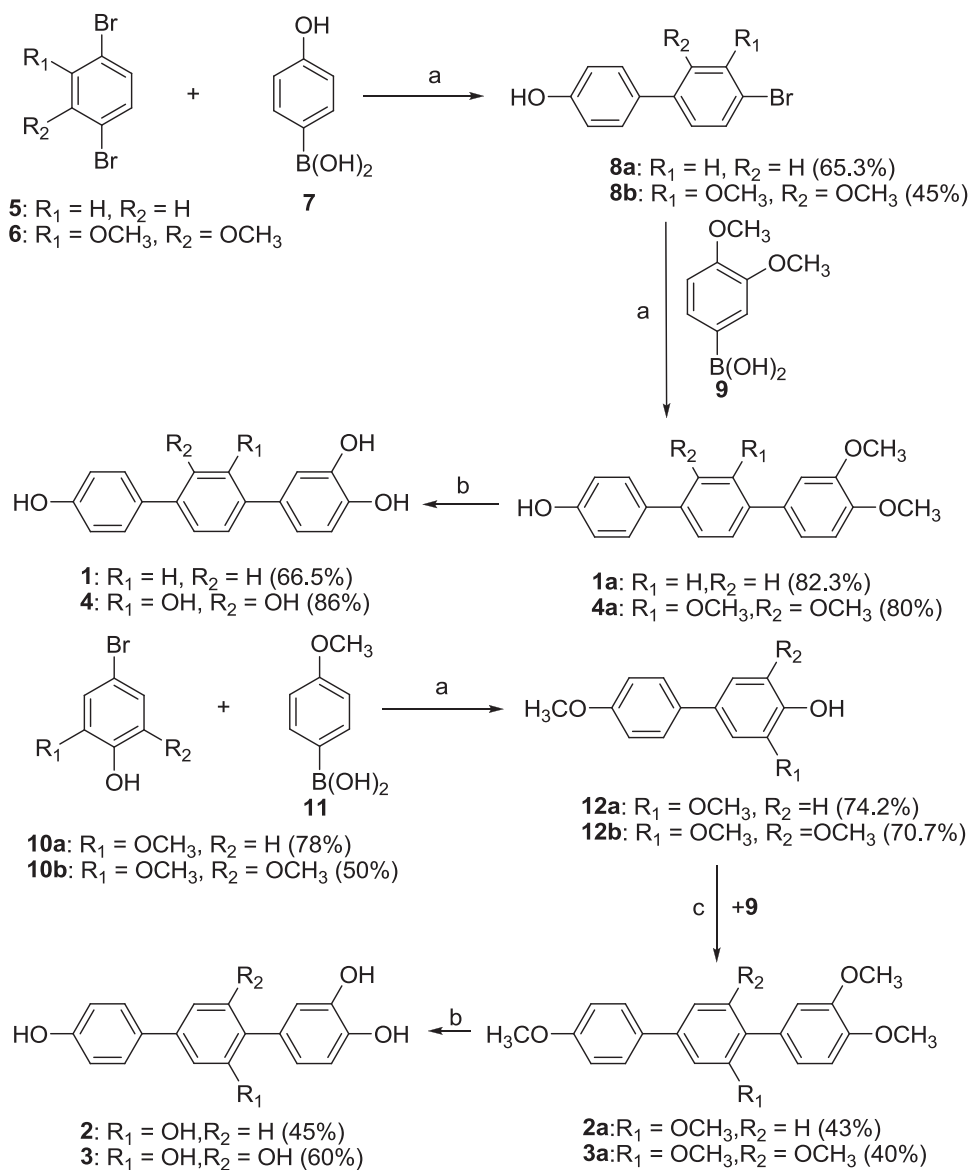
To examine the activity status of these DNA damage-sensing proteins, Western blot analysis was performed using phospho-specific antibodies. As shown in Fig. 2B, Etoposide, a DNA-damaging agent, increased the phosphorylation levels of Ser1981 at ATM, then led to an opening proceed of downstream target, Ser139 at H2AX. The level of p53 increased after treatment with Etoposide for 12 h both in common state and phosphorylation at Ser15. In contrast, the phosphorylation levels of these proteins did not change in MDA-MB-435 cells treated with compound **1**. These data suggested that compound **1** did not produce DNA damage.

To study the molecular basis of compound **1** mediated growth arrest in MDA-MB-435 cells, the expression of known G2/M-associated proteins were examined in MDA-MB-435 cells after being treated with compound **1** using Western blot analysis. As shown in Fig. 2B, after 12 h of compound **1** treatment, the MDA-MB-435 cells showed a significant increase of cyclin B and cdc2 protein, and the protein level was gradually enhanced up during 24 h. On the contrary, GADD45 $\alpha$ , cdc25c, and myt1 markedly decreased in compound **1**-treated MDA-MB-435 cells.

Cell morphological observations were subsequently performed to investigate the nature of cell death induced by compound **1**. With the gradient enhancement of drug concentration, a large proportion of cells became round in shape and dead, while the untreated cells displayed normal shapes and clear skeletons under the same conditions (Fig. 3A). Chromatin condensation and nuclear fragmentation were also observed by the DAPI staining, which typically occurred during apoptosis (Fig. 3A).

To further characterize the apoptosis induced by compound **1**, an Annexin V/PI assay was used to quantitate the apoptotic cells of MDA-MB-435. As illustrated in Fig. 3B, the proportion of Annexin V and PI-positive (apoptotic) cells increased from 0.61% to 12.87% when they were exposed to  $2 \mu M$  of compound **1** for 24 h. Collectively, these data confirmed that compound **1** induced MDA-MB-435 cell apoptosis.

We subsequently evaluated whether compound **1** induced apoptosis in a caspase-dependent manner. To serve this purpose, the impact of compound **1** on procaspase-3 (an indicator of caspase-3 activity) and PARP (a downstream target of caspase) were preferentially examined. The results showed that compound **1** dose-dependently decreased the expression of procaspase-3 and increased the expression of cleaved-caspase-3 in MDA-MB-435



Reagents and conditions: (a) Pd-DPPF, KF, Dioxane, 2~28 h. (b)  $\text{BBr}_3$ ,  $\text{CH}_2\text{Cl}_2$ ,  $-78^\circ\text{C}$ , >18 h. (c) 1.  $\text{CH}_2\text{Cl}_2$ , 10% aqueous NaOH, triflic anhydride,  $0^\circ\text{C}$ ; 2. Pd-DPPF, KF, Dioxane, 2~28 h.

**Scheme 1.** Synthesis route of compounds **1–4** and **1a–4a**.

cells after 24 h of incubation time (Fig. 3C). In addition, compound **1** resulted in PARP cleavage in a dose-dependent fashion as evidenced by an increase in 85 kDa of inactive intermediate band of PARP and a concomitant decrease in 116 kDa of the full length (Fig. 3C).

Induction of apoptosis can be triggered by inhibition of anti-apoptotic and/or activation of pro-apoptotic mechanisms. Bcl-2 family proteins, including anti-apoptotic members (such as Bcl-2) and pro-apoptotic members (such as Bax, Bak), play a pivotal role in apoptotic response [12]. It is well known that the ratio of Bax/Bcl-xL determines the apoptotic fate of cells and an increase in that ratio predicts that the cells will undergo apoptosis. As shown in Fig. 3C, the expression level of anti-apoptotic Bcl-2 was sensibly affected by the treatment with compound **1** after 12 h, while Bax and Bak were inversely regulated.

### 2.2.3. DNA topoisomerases inhibition

In our previous work, natural *p*-terphenyl derivatives have been shown to induce generation of ROS in MDA-MB-435 cells [8]. However, the antioxidant N-acetylcysteine (NAC), a direct scavenger of ROS, was unable to inhibit the cell cycle arrest and apoptosis induced by compound **1** (Supplemental Fig. 1). This result suggested that intracellular ROS generation was not related to compound **1** inducing cell cycle arrest and apoptosis in MDA-MB-435 cells.

Topoisomerases are involved in regulating the under- and over-winding of DNA. This process is essential for removing knots and tangles in the DNA, without which cells can be dead. It has been established that strategic interference with enzymes is effective for cancer therapy [3]. Therefore, a DNA relaxation assay was performed to evaluate the Topo inhibition activity of compound **1**.

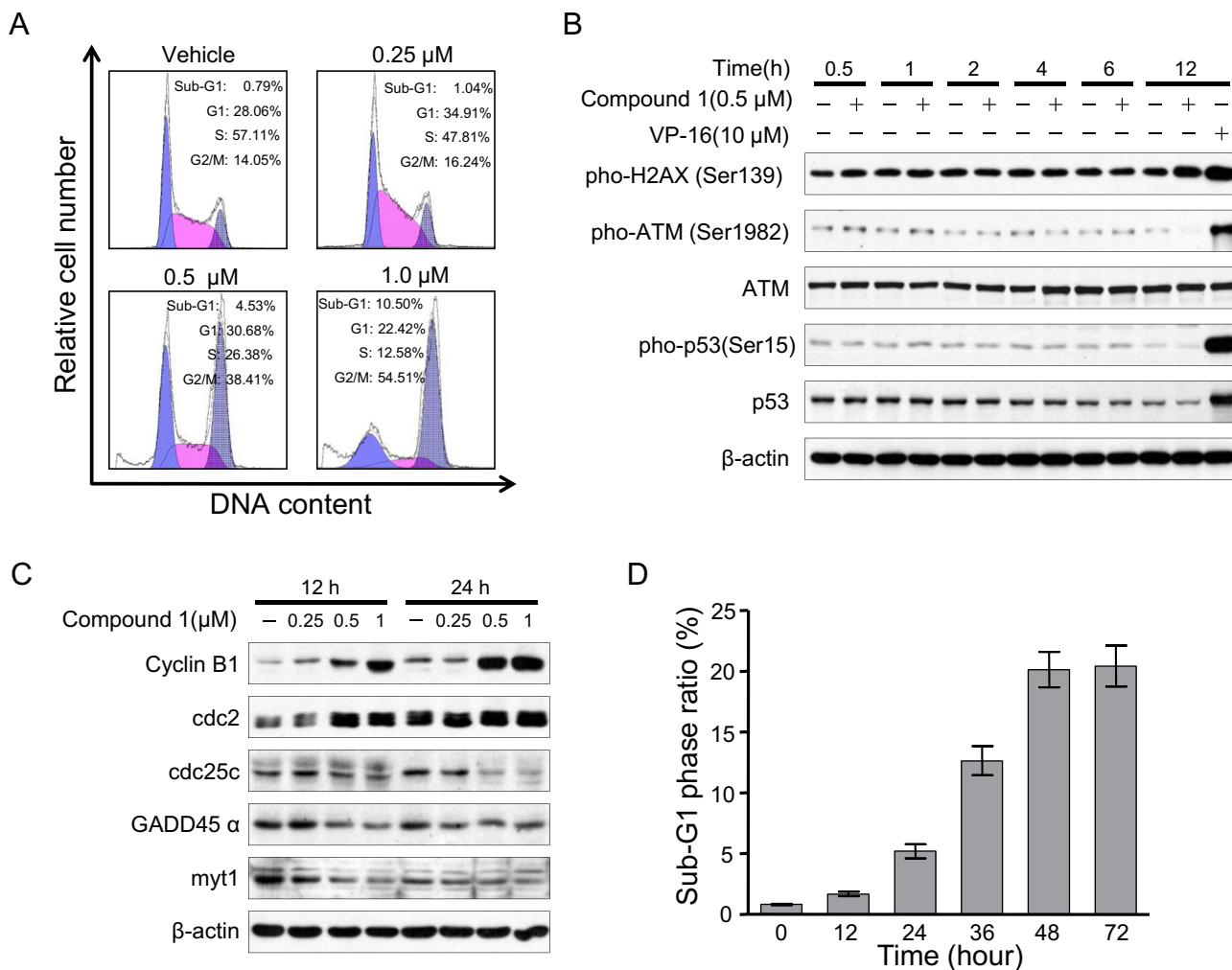


**Fig. 2.** Effect of compound **1** on cell cycle progression. (A) MDA-MB-435 cells were treated with increasing concentrations of compound **1** for 24 h and analyzed for propidium iodide (PI) stained-DNA content by flow cytometry. Values indicated the percentages of the cell population at the phase of the cell cycle. Results were representative of three independent experiments. (B) Western blot analysis for the activations of DNA damage-sensing proteins in MDA-MB-435 cells. The phosphorylations of ATM at Ser1981, H2AX at Ser139, p53 at Ser15, and the expressions of p53 and ATM were determined by Western blotting in MDA-MB-435 cells after the cells were treated with compound **1** for indicated time. (C) Expression of cell cycle arrest-related proteins in MDA-MB-435 cells treated with compound **1**. The levels of cell cycle-related proteins including CDC25, Cyclin B1 and CDK1 were assessed by western blot assay. Equal loading of protein was confirmed by stripping and reprobing the blots with  $\beta$ -actin. (D) Flow cytometric analysis of compound **1**-induced cell death in MDA-MB-435 cells. MDA-MB-435 cells were treated with compound **1** and analyzed by flow cytometry. The population of cells in the sub-G1 phase represented cellular fragments due to apoptosis. The data shown were representative of three independent experiments. Data shown are the mean + SD of three independent experiments.

In the absence of compound **1**, the supercoiled plasmid pBR322 was completely relaxed evidenced by the visualization of its slower migration rate through agarose gel electrophoresis (Fig. 4A). In contrast, with the increasing concentration of compound **1**, an increasing amount of supercoiled pBR322 was observed in the agarose gel, which was distinct from other relaxed plasmid due to its faster migration rate. Similar results were obtained for Topo II $\alpha$  activity inhibition (Fig. 4A). These results confirmed that compound **1** inhibited the activity of Topo I and Topo II $\alpha$ .

Compound **1** was confirmed to inhibit both Topo I and II $\alpha$  from the above assays, and we next studied the mode of inhibition. Topoisomerase inhibitors could be classified as topo poisons and topo catalytic suppressors. The former acted by stabilizing DNA cleavable enzyme complexes leading to DNA break. On the contrary, the latter acted by stabilizing enzyme, so DNA strands remain intact and no DNA breaks occur. By detecting the presence or absence of the DNA breaks, Topo poisons therefore could be distinguished from Topo catalytic suppressors [13,14].

Circular supercoiled plasmid (SC) DNA was used as the substrate in the inhibition mode assay. If a compound was a Topo suppressor, the DNA starting material would remain intact because the topoisomerase catalyzed cleavage of DNA was blocked by the suppressor. If a compound was a Topo poison, the DNA cleavage would occur in the presence of the enzyme. Subsequently, the cleaved DNA products would be stabilized by poisons through the formation of a cleavable enzyme-inhibitor-DNA complex. Thereafter, the cleaved DNA products NOC (nicked open circular) DNA for Topo I and L (linear) DNA for Topo II $\alpha$ , could be trapped by sodium dodecyl sulfate (SDS). Subsequent proteinase K removes the bound enzymes. After the resolution of DNA species by gel electrophoresis, the presence or absence of the NOC DNA band would classify the inhibitor as a Topo I poison or suppressor, the same as the presence or absence of the L DNA band for Topo II $\alpha$  [15]. As illustrated in Fig. 4B, at a concentration of 100  $\mu$ M, neither NOC DNA nor L DNA band was observed for compound **1**. This indicated that compound **1** was a Topo suppressor, not a poison. In contrast, NOC DNA and L

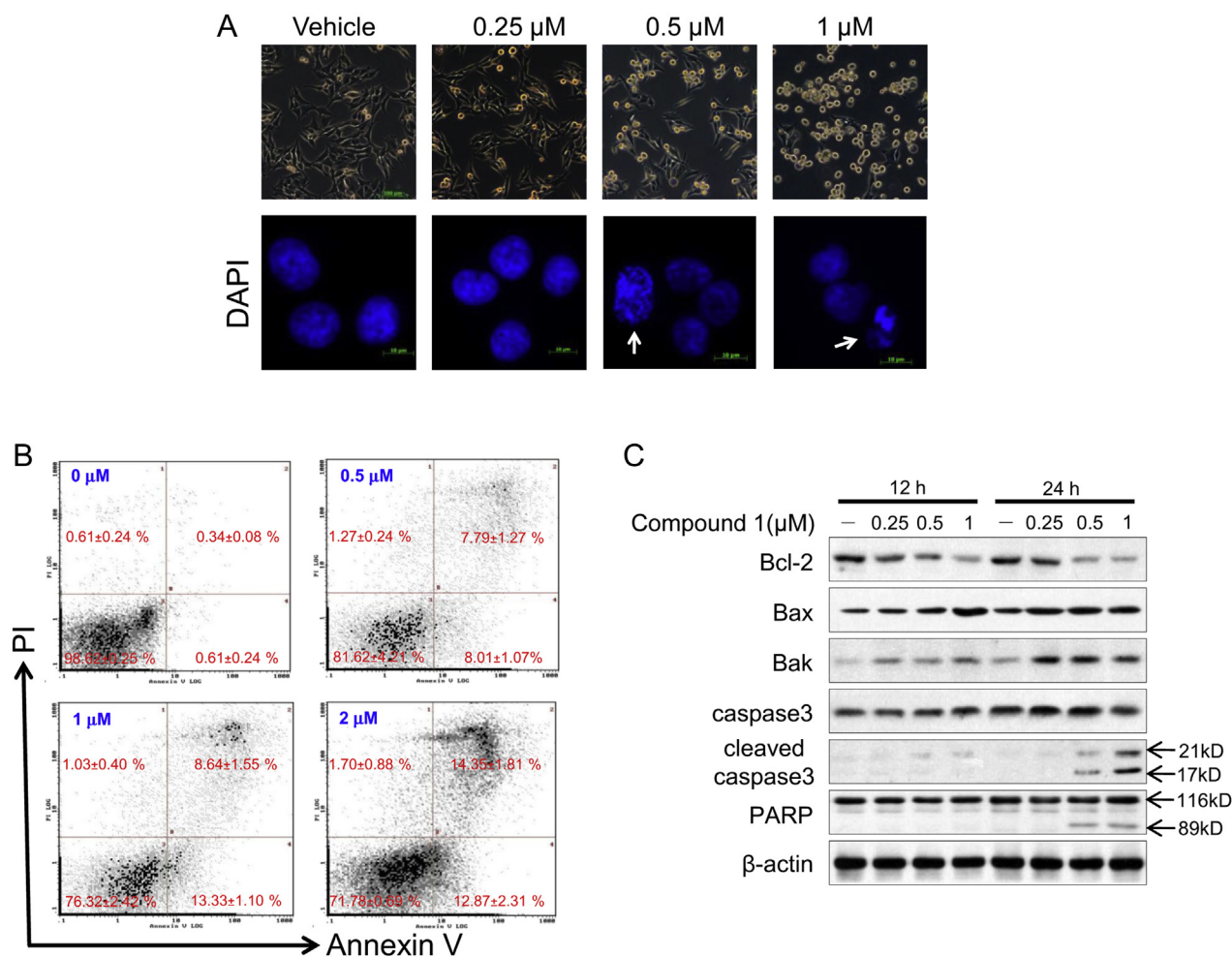


**Fig. 3.** Compound **1** induced apoptosis in MDA-MB-435 cells. (A) Compound **1** induced apoptosis in MDA-MB-435 cells with DAPI staining. MDA-MB-435 cells were treated with different concentrations of Compound **1**. Then, the cells were harvested and stained with DAPI in PBS and examined by a fluorescence microscopy (scale bar is 10  $\mu\text{m}$ ). (B) Flow cytometric analysis by Annexin-V/PI double-staining. MDA-MB-435 cells were treated with indicated concentrations of compound **1** for 24 h and stained with annexin V-FITC/PI to analyze apoptotic and necrotic cell population as described earlier. Data were representative of one of the three similar experiments. (C) Effects of compound **1** on the expression of apoptotic relating-proteins. MDA-M caspase-3, full-length PARP (116-kDa) and cleaved PARP (85-kDa) indicated by B-435 cells were treated with compound **1** for the indicated times. Whole cell lysates were prepared and signals of processed proteins were detected by Western blotting with antibodies specific to Bcl-2, Bak, Bad, caspase3, cleaved caspase-3 and PARP. Cleaved caspase-3, full-length PARP (116-kDa) and cleaved PARP (85-kDa) were indicated by arrows.  $\beta$ -actin was used as an internal loading control. Data shown were representative of three independent experiments with similar results.

DNA were clearly observed for positive control compounds, OPT (Fig. 4B, lane 5) for Topo I, and VP-16 (Fig. 4B, lane 6) for Topo II $\alpha$ .

DNA intercalation is an important feature of some Topo inhibitors such as adriamycin and amsacrine, which can bind to the minor groove of DNA and produce positively supercoiled DNA in the presence of topoisomerases [16]. Therefore, the intercalating ability of compound **1** into DNA was assessed by a Topo I-catalyzed DNA unwinding assay, which is based on the ability of intercalating compounds to unwind the DNA duplex and thereby change the DNA twist [17]. As shown in Fig. 4C, in the presence of a strongly intercalative drug such as EB and PI, a net negative supercoiling of relaxed substrate DNA was induced (lanes 7 and 8). Conversely, no unwinding was observed with the non-intercalative drug OPT (lanes 3). Compound **1** also showed no unwinding effect on DNA up to 100  $\mu\text{M}$  (lanes 4–6). The results indicated that compound **1** had no significant DNA intercalating activity.

The topoisomerases inhibitory activities of other analogs were also evaluated by the DNA relaxation assay. Hydroxycamptothecin (OPT) and etoposide (VP-16), two well-known Topo I and Topo II $\alpha$  inhibitors, were used as positive control respectively. As shown in

Fig. 5A and B, after treatment with 100  $\mu\text{M}$  compound **1**, **2**, **3** and **4** only compound **1** and **3** had been found to inhibit the enzymatic activity of Topo I in a way similar to that of known Topo I inhibitors (OPT, 100  $\mu\text{M}$ ). On the contrary, compound **1a**, **2a**, **3a** and **4a** showed no remarkable inhibition of Topo I and Topo II $\alpha$  catalytic activity at 100  $\mu\text{M}$ . These data suggested there was certain correlation between cytotoxicity and Topo inhibition. The analogs (**2** and **4**) with lower potency against Topo I still exhibited similar cytotoxicity compared to the ones (**1** and **3**) with higher potency against Topo I. The fact that the cytotoxicity was mainly related to Topo II $\alpha$  inhibition for this class of compounds could be concluded. Additionally, MDA-MB-435 cell line, in which Topo I was highly expressed [18,19], was more sensitive to compounds **1–4** than other two cell lines. This data provided indirect support for the conclusion. The solvent DMSO has no effect on the results (data not shown).

The Topo II $\alpha$  inhibition of compounds **1–4**, **1a–4a** was further confirmed by Topo II $\alpha$  mediated kDNA decatenation assays. As shown in Fig. 5C, compound **2** and **4** apparently suppressed Topo II mediated decatenation of kDNA at the concentration of 100  $\mu\text{M}$ .

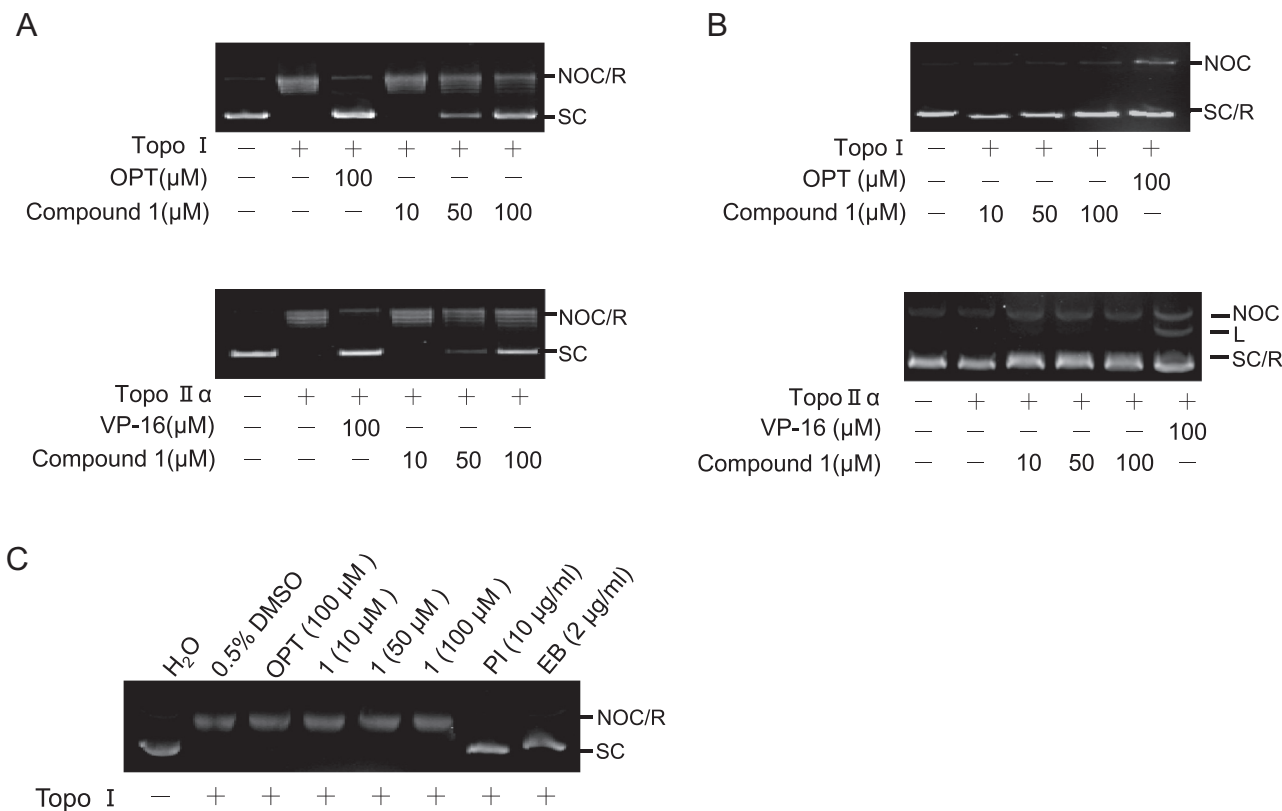


**Fig. 4.** Inhibitory effect of compound **1** on Topo I and Topo II $\alpha$  mediated DNA relaxation. (A) Compound **1** inhibited Topo I/II $\alpha$ -mediated supercoiled DNA relaxation. Negatively supercoiled pBR322 (SC) and relaxed DNA (R) were shown by electrophoresis on an agarose gel after compound **1** treatment at the indicated concentration. OPT and VP-16 were used at 100  $\mu$ M as the positive control. (B) Effects of compound **1** on the Topo I/II $\alpha$ -mediated DNA cleavage. Negatively supercoiled pBR322 (lane 1) was shown for reference. The position of linear DNA (L) and nicked open circular (NOC) were indicated. (C) Effects of compound **1** on the DNA unwinding assay with Topo I. Lane 1, pBR322 DNA only. Lane 2, pBR322 DNA and Topo I. Lanes 3–8, pBR322 DNA, Topo I, and various concentrations of compound **1**. PI and EB were used as the positive control.

While compound **1** and compound **3** exhibited partial inhibition of Topo II $\alpha$ . Almost no decatenation activity was observed in the presence of compounds **1a**, **2a**, **3a** and **4a**.

### 3. Discussion

Currently, most of the topoisomerase inhibitors show selective inhibition against either Topo I or Topo II, and only a small amount of compounds is capable of inhibiting both the two enzymes above. Selective inhibition of the Topo I enzyme can, however, induce a reactive increase in Topo I levels and vice versa. This mechanism is associated with the development of drug resistance. Therefore, searching for new compounds that inhibit both Topo I and Topo II is very important because of the deficiency of specific inhibitors which can overcome multidrug resistance (MDR) cancer cells [20]. In this study, compound **1**, showing significant anticancer activities, strongly inhibited the enzymatic activity of Topo I and Topo II $\alpha$  (Fig. 4). In contrast, compound **2** and **4**, with less anticancer activities than compound **1**, showed selective inhibition against Topo II $\alpha$  (Fig. 5).

Despite their efficiency in the clinics, current anticancer therapies with topoisomerase inhibitors are limited by certain considerably negative consequences. The most negative consequence from observation is that the treatment with Topo poisons may result in secondary malignancies [21]. However, compound **1** did not induce Topo-mediated DNA cleavage in our experiments (Fig. 4B). DNA-unwinding assay indicated that compound **1** had no significant DNA intercalating activity (Fig. 4C). Pre-incubation of

compound **1** with the enzyme prior to the addition of DNA increased the inhibitory activity.

In eukaryotes, G2/M phase, a highly complex multistage process, is a critical phase before cell division during the cell cycle. An important event prior to mitotic entry is the decatenation of sister chromatids, which are highly entangled as a consequence of DNA replication. This process is carried out by DNA topoisomerase [22,23]. Although compound **1** did not produce DNA strand breaks, it caused a cell cycle arrest at the G2/M phase on cell cycle just as Topo I poisons (Fig. 2A). This effect could be due to the fact that Topo II was perturbed by compound **1**, resulting in catenation of sister chromatids which could then lead to the G2/M delay. Cyclin B, in association with cdc2 (CDK1), governs cell cycle progression by enhancing cell cycle distribution in the G2/M fraction. The inhibition of cyclin B/cdc2 complexes prevents the G2/M transition [24]. However, our data showed that compound **1** increased the level of cyclin B/cdc2 (Fig. 2C). This property might also be due to Topo I inhibition, which led to the spindle checkpoint activation and mitotic exit prevention [25].

The arrest of cell cycle progression at G2/M phase provides an opportunity for cells to either undergo repair mechanisms or follow the apoptosis. In this study, increasing percentages of apoptosis were observed when the cells were sorted by FACS after exposed to compound **1** (Fig. 2A), while the time-dependent induction of a sub-G1 cell population suggested that G2/M-phase arrest might be an inverse process leading to apoptosis (Fig. 2D). The apoptosis was further confirmed by nuclear fragmentation staining (DAPI staining) and Annexin V/PI staining of compound **1**-treated cells (Fig. 3A&B). There are two distinct apoptotic pathways in mammals,

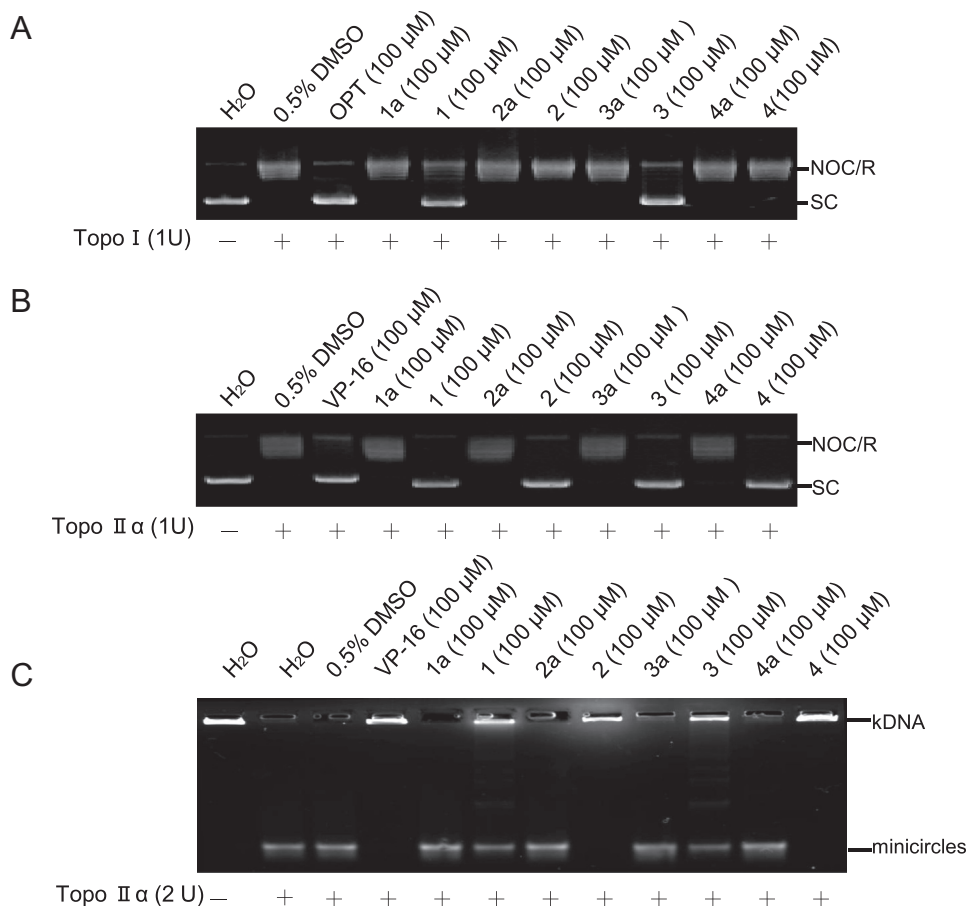


**Fig. 5.** Effects of *p*-terphenyls derivatives on the Topo I/II $\alpha$ -mediated supercoiled DNA relaxation. (A): Topo I; (B): Topo II $\alpha$ . Lane 1, pBR322 DNA only. Lane 2, pBR322 DNA and Topo I/II $\alpha$ . Lanes 3–11, pBR322 DNA, Topo I/II $\alpha$ , and various compounds (100  $\mu$ M). OPT and VP-16 were used as the positive control; (C) Topo II $\alpha$  mediated kDNA decatenation assay. kDNA was used as substrate, the position of kDNA and decatenation products minicircles was indicated.

the mitochondrial pathway and the death receptor pathway. The activation of caspase-3 plays a crucial role in the initiation of apoptosis. Our data showed that compound **1** induced PARP cleavage and the activation of caspase-3. Furthermore, the ratio of Bcl-2/Bax (Fig. 3C), which is crucial for the activation of the mitochondrial apoptotic pathway, decreased in cells treated with compound **1**. Taken together, these results indicated that compound **1** activated caspase-dependent apoptosis in MDA-MB-435 cells mainly *via* mitochondrial pathway.

In summary, eight new *p*-terphenyls derivatives were successfully synthesized. Some of these compounds exhibited potent anticancer activity, which were mainly related to Topo II $\alpha$  inhibition ability. Our study also identified that compound **1** was a novel kind of Topo I and Topo II $\alpha$  catalytic inhibitor. The biological properties of compound **1** showed its potential as a novel cancer chemotherapeutic agent.

## 4. Experimental section

### 4.1. Chemistry

All melting points were determined on a micro melting point apparatus and were uncorrected.  $^1\text{H}$  NMR and  $^{13}\text{C}$  NMR spectra were obtained on a Bruker Avance-600 NMR-spectrometer or Inova-600 NMR-spectrometer in the indicated solvents. Chemical shifts are expressed in ppm ( $\delta$  units) relative to TMS signal as internal reference. TLC was performed on Silica Gel GF254 and spots

were visualized by iodine vapors or by irradiation with UV light (254 nm). Flash column chromatography was performed on column packed with Silica Gel 60 (200–300 mesh). Solvents were reagent grade and, when necessary, they were purified and dried by standard methods. Concentration of the reaction solutions involved the use of rotary evaporator at reduced pressure.

#### 4.1.1. 4-Bromo-2-methoxyphenol (**10a**) [26]

A solution of NBS (1 eq.) in DMF (50 mL) was added dropwise to a solution of guaiacol (1 eq.) in DMF (50 mL) at 0  $^{\circ}\text{C}$ . After being stirred for 30 min, the reaction mixture was quenched with ice water and extracted with ethyl acetate. The combined organic layers were washed with brine, dried over anhydrous sodium sulfate and then evaporated to dryness under reduced pressure. The residue was further purified by column chromatography over Silica Gel 200–300 N (petroleum ether/ethyl acetate 9.5:0.5) to give **10a** as an oil (78%).

#### 4.1.2. 3,6,6-tribromo-2-hydroxycyclohex-2-enone

The cyclohexanone (1 eq.) with  $\text{CuBr}_2$ , 30 times as much as that, in 50% dioxane (v/v, 200 mL) was refluxed for 3 h. Afterward, the reaction mixture was quenched with water and extracted with ethyl acetate. The organic layer was washed with brine, dried over anhydrous sodium sulfate and evaporated to dryness under reduced pressure. The residue was purified by column chromatography using petroleum ether/ethyl acetate 20:1 to give 3,6,6-tribromo-2-hydroxycyclohex-2-enone [27] (28%).

#### 4.1.3. 3,6-dibromobenzene-1,2-diol

The 3,6,6-tribromo-2-hydroxycyclohex-2-enone (1 eq.) was stirred with LiCO<sub>3</sub> (1.5 eq.) in DMF (20 mL) for 2 h in a nitrogen atmosphere at 30 °C. After the reaction finished, the mixture was quenched with water and extracted with ethyl acetate. The organic layer was washed with 5% HCl and brine, dried over anhydrous sodium sulfate and evaporated to dryness. The residue was further purified by column chromatography using petroleum ether/ethyl acetate 2:1 to give 3,6-dibromobenzene-1,2-diol [28] (65%).

#### 4.1.4. 1,4-dibromo-2,3-dimethoxybenzene (**6**) [29]

A solution of 3,6-dibromobenzene-1,2-diol (1.0 eq.) in acetone (10 mL) was added to the mixture of dimethyl sulfate (4.0 eq.) and K<sub>2</sub>CO<sub>3</sub> (4.0 eq.). After being stirred overnight, the mixture was quenched with sufficient quantum aqueous ammonia and extracted with ethyl acetate. The aqueous layer was washed with ethyl acetate. The organic phases were combined, washed with brine, dried over anhydrous sodium sulfate and evaporated to dryness under reduced pressure. The crude product was purified by chromatography using petroleum ether/ethyl acetate 20:1 to yield the corresponding derivatives 1,4-dibromo-2,3-dimethoxybenzene (95%). <sup>1</sup>H NMR (600 MHz, DMSO-*d*<sub>6</sub>) δ 7.35 (s, 2H), δ 3.83 (s, 6H).

#### 4.1.5. 4-Bromo-2,6-dimethoxyphenol (**10b**) [30]

2,6-dimethoxyphenol (1 eq.), sodium hydride (0.01 eq., 60% in mineral oil), and anhydrous MeOH (1.2 mL) in 150 mL of anhydrous CH<sub>2</sub>Cl<sub>2</sub> were treated with N-bromosuccinimide (1 eq.) at -45 °C. The products were evaporated under reduced pressure. The residue was purified by column chromatography over Silica Gel 200–300 N (petroleum ether/ethyl acetate 9:1) to give white crystals (50%).

#### 4.1.6. General parallel procedure a (Scheme 1) for the synthesis of Compound **1a**, **3a**, **8a**, **8b**, **12a** and **12b**

The appropriate bromo derivatives (1 eq.), appropriate phenyl boronic acids **7/9/11** (1.5 eq.) and KF (3.0 eq.) were dissolved respectively in dioxane, and the three resulting mixtures were deoxygenated with a stream of N<sub>2</sub>. After 10 min, PdCl<sub>2</sub>(dppf) (0.05 eq.) was added, and each mixture was brought to reflux, allowed to be stirred under N<sub>2</sub> for 5–22 h until the reaction is complete, which was detected by TLC. Then each solution was cooled to room temperature. After that, each solution was poured into a mixture of H<sub>2</sub>O and ethyl acetate, and the two phases were separated. The aqueous layer was washed with ethyl acetate, and the organic phases were combined and washed with brine. The ethyl acetate layer was dried over anhydrous sodium sulfate and evaporated to dryness under reduced pressure. Purification of each crude product by chromatography using petroleum ether/ethyl acetate 4:1 or 9:1 yielded the corresponding derivatives of **1a**, **3a**, **8a** [31], **8b**, **12a** [32]: <sup>1</sup>H NMR (600 MHz, DMSO-*d*<sub>6</sub>) δ 9.01 (s, 1H), 7.53 (d, *J* = 8.4 Hz, 2H), 7.12 (s, 1H), 7.01 (d, *J* = 8.4 Hz, 1H), 6.97 (d, *J* = 8.4 Hz, 2H), 6.82 (d, *J* = 8.4 Hz, 1H), 3.8 (s, 3H), 3.65 (s, 3H), and **12b** [33].

#### 4.1.7. General parallel procedure b (Scheme 1) for the synthesis of compounds **1**, **2**, **3**, and **4**

The **1a**, **2a**, **3a**, and **4a** (1 eq.) were dissolved respectively in anhydrous CH<sub>2</sub>Cl<sub>2</sub> (1 mL) at -78 °C. Then BBr<sub>3</sub> (3 eq.) was added to each solution, and the four resulting reaction mixtures were allowed to warm to room temperature for 20 h and treated as follows. Each solution was poured into ice water followed by being warmed to ambient temperature, and then each solution was washed twice with ethyl acetate. The combined organic layer was dried over anhydrous sodium sulfate and evaporated to dryness under reduced pressure [34]. Purification of each crude product by

chromatography using CH<sub>2</sub>Cl<sub>2</sub>/ethyl acetate 9:1 yielded the corresponding derivatives.

#### 4.1.8. General parallel procedure c (Scheme 1) for the synthesis of compounds **2a** and **3a**

Intermediate **12a** or **12b** was dissolved respectively in a biphasic mixture of CH<sub>2</sub>Cl<sub>2</sub> and 10% aqueous NaOH followed by slow addition of triflic anhydride (3 eq.) at 0 °C. After finishing dropping, the mixture was allowed to warm to room temperature and stirred for 30 min. Two phases were separated and the CH<sub>2</sub>Cl<sub>2</sub> layer, washed with brine, was evaporated to dryness under reduced pressure, the crude product of the steps above was used directly in the next step [35]. Then, the crude product, phenyl boronic acid **2** (2 eq.) and KF (3.0 eq.) were dissolved in dioxane respectively, and the resulting mixtures were deoxygenated with a stream of N<sub>2</sub>. After being stirred for 10 min, PdCl<sub>2</sub>(dppf) (0.05 eq.) was added, and each mixture was brought to reflux, allowed to stir under N<sub>2</sub> for 5–28 h until the reaction, detected by TLC, was complete. Then each mixture was cooled to the room temperature and treated as follows. Each solution was poured into a mixture of H<sub>2</sub>O and ethyl acetate, and the two phases were separated. The aqueous layer was washed with ethyl acetate. The organic phases were combined and washed with brine. The ethyl acetate phase was dried over anhydrous sodium sulfate and evaporated to dryness under reduced pressure. Purification of each crude product by chromatography using petroleum ether/ethyl acetate 4:1 or 9:1 yielded the corresponding derivatives.

#### 4.1.9. [1,1':4',1''-Terphenyl]-4''-monol,3,4-dimethoxy (**1a**)

Mp 250–252 °C; <sup>1</sup>H NMR (600 MHz, DMSO-*d*<sub>6</sub>) δ 3.77 (s, 3H, OCH<sub>3</sub>), 3.92 (s, 3H, OCH<sub>3</sub>), 6.87 (d, *J* = 8.4 Hz, 2H, H3'', H5''), 7.04 (d, *J* = 8.4 Hz, 1H, H5), 7.23 (d, *J* = 8.4 Hz, 1H, H6), 7.26 (s, 1H, H2), 7.54 (d, *J* = 8.4 Hz, 2H, H2', H6'), 7.64 (d, *J* = 8.4 Hz, 2H, H3', H5'), 7.71 (d, *J* = 8.4 Hz, 2H, H2'', H6''), 9.59 (s, 1H, OH); <sup>13</sup>C NMR (600 MHz, CDCl<sub>3</sub>) δ 55.39 (OCH<sub>3</sub>), 55.42 (OCH<sub>3</sub>), 109.99 (C5), 112.0 (C2), 115.6 (C3''), 115.6 (C5''), 118.4 (C6), 126.1 (C2'), 126.1 (C6'), 126.6 (C3'), 126.6 (C5'), 127.5 (C2''), 127.5 (C6''), 130.3 (C1), 132.4 (C1''), 137.9 (C1'), 138.4 (C4'), 148.3 (C4), 148.9 (C3), 157.0 (C4''); HRMS (ESI) Calcd. for C<sub>20</sub>H<sub>19</sub>O<sub>3</sub> [M + H]<sup>+</sup> 307.1334, Found: 307.1329.

#### 4.1.10. [1,1':4',1''-Terphenyl]-3,4,4''-triol (**1**)

Mp > 260 °C; <sup>1</sup>H NMR (600 MHz, DMSO-*d*<sub>6</sub>) δ 6.82 (d, *J* = 8.4 Hz, 1H, H5), 6.85 (d, *J* = 8.4 Hz, 2H, H3'', H5''), 6.97 (d, *J* = 8.4 Hz, 1H, H6), 7.06 (s, 1H, H2), 7.51 (d, *J* = 8.4 Hz, 2H, H2', H6'), 7.55 (d, *J* = 7.8 Hz, 2H, H3', H5'), 7.60 (d, *J* = 7.8 Hz, 2H, H2'', H6''), 9.02 (s, 1H, OH), 9.05 (s, 1H, OH), 9.54 (s, 1H, OH); <sup>13</sup>C NMR (600 MHz, (CD<sub>3</sub>)<sub>2</sub>CO) δ 113.7 (C5), 113.7 (C2), 115.7 (C3''), 115.7 (C5''), 118.2 (C2'), 118.2 (C6'), 126.5 (C3'), 126.5 (C5'), 126.6 (C6), 127.7 (C2''), 127.7 (C6''), 131.9 (C1), 132.7 (C1''), 138.99 (C1'), 139.1 (C4'), 144.9 (C4), 145.4 (C3), 157.1 (C4''); HRMS (ESI) Calcd. for C<sub>18</sub>H<sub>15</sub>O<sub>3</sub> [M + H]<sup>+</sup> 279.1021, Found: 279.1108.

#### 4.1.11. [1,1':4',1''-Terphenyl]-2',3',4,4''-tetramethoxy (**2a**)

Mp 131–132 °C; <sup>1</sup>H NMR (600 MHz, CDCl<sub>3</sub>) δ 3.87 (s, 3H, OCH<sub>3</sub>), 3.89 (s, 3H, OCH<sub>3</sub>), 3.92 (s, 3H, OCH<sub>3</sub>), 3.93 (s, 3H, OCH<sub>3</sub>), 6.94 (d, *J* = 9 Hz, 1H, H5), 7.00 (d, *J* = 8.4 Hz, 2H, H3'', H5''), 7.12 (d, *J* = 1.8 Hz, 1H, H3'), 7.14 (s, 1H, H2), 7.15 (d, *J* = 9 Hz, 1H, H6), 7.21 (dd, *J* = 7.8, 1.8 Hz, 1H, H5'), 7.37 (d, *J* = 7.8 Hz, 1H, H6'), 7.58 (d, *J* = 8.4 Hz, 2H, H2'', H6''); <sup>13</sup>C NMR (600 MHz, CDCl<sub>3</sub>) δ 159.2 (C4''), 156.6 (C2'), 148.3 (C3), 148.1 (C4), 141.2 (C4'), 133.5 (C1''), 130.93 (C1), 130.87 (C1'), 128.8 (C6'), 128.1 (C2''), 128.1 (C6''), 121.8 (C6), 119.2 (C5'), 114.2 (C3''), 114.2 (C5''), 112.9 (C2), 110.8 (C3'), 109.8 (C5), 55.9 (OCH<sub>3</sub>), 55.9 (OCH<sub>3</sub>), 55.7 (OCH<sub>3</sub>), 55.4 (OCH<sub>3</sub>); HRMS (ESI) Calcd. for C<sub>22</sub>H<sub>23</sub>O<sub>4</sub> [M + H]<sup>+</sup> 351.1600, Found: 351.1595.

#### 4.1.12. [1,1':4',1''-Terphenyl]-2',3,4,4''-tetol (**2**)

Mp > 260 °C; <sup>1</sup>H NMR (600 MHz, DMSO-*d*<sub>6</sub>) δ 6.75 (d, *J* = 7.8 Hz, 1H, H5), 6.83 (br, 3H H5' H3'', H5''), 7.03 (br, 2H, H6, H2), 7.07 (s, 1H, H3'), 7.20 (d, *J* = 7.2 Hz, 1H, H6'), 7.41 (d, *J* = 7.2 Hz, 2H, H2'', H6''), 8.86 (s, 2H, OH), 9.41 (s, 1H, OH), 9.54 (s, 1H, OH); <sup>13</sup>C NMR (600 MHz, DMSO-*d*<sub>6</sub>) δ 113.8 (C5), 115.7 (C2), 116.1 (C3''), 116.1 (C5''), 117.1 (C3'), 117.6 (C5'), 120.4 (C6), 126.6 (C6'), 127.8 (C2''), 127.8 (C6''), 129.9 (C1'), 130.7 (C1), 131.2 (C1''), 140.0 (C4'), 144.6 (C3), 145.0 (C4), 154.8 (C2'), 157.5 (C4''); HRMS (ESI) Calcd. for C<sub>18</sub>H<sub>15</sub>O<sub>4</sub> [M + H]<sup>+</sup> 295.0970, Found: 295.0967.

#### 4.1.13. [1,1':4',1''-Terphenyl]-2',3,4,4'',6'-pentamethoxy (**3a**)

Mp 170–172 °C; <sup>1</sup>H NMR (600 MHz, CDCl<sub>3</sub>) δ 3.81 (s, 6H, OCH<sub>3</sub>), 3.87 (s, 3H, OCH<sub>3</sub>), 3.88 (s, 3H, OCH<sub>3</sub>), 3.91 (s, 3H, OCH<sub>3</sub>), 6.81 (s, 2H, H3', H5'), 6.94 (d, *J* = 8.4 Hz, 1H, H5), 6.96 (d, *J* = 1.8 Hz, 1H, H2), 6.97 (dd, *J* = 8.4, 1.8 Hz, 1H, H6), 7.00 (d, *J* = 9 Hz, 2H, H3'', H5''), 7.58 (d, *J* = 9 Hz, 2H, H2'', H6''); <sup>13</sup>C NMR (600 MHz, CDCl<sub>3</sub>) δ 55.4 (OCH<sub>3</sub>), 55.7 (OCH<sub>3</sub>), 55.8 (OCH<sub>3</sub>), 56.0 (OCH<sub>3</sub>), 56.0 (OCH<sub>3</sub>), 103.1 (C3'), 103.1 (C5'), 110.5 (C1'), 114.2 (C3''), 114.2 (C5''), 114.3 (C5), 117.6 (C2), 123.2 (C6), 126.2 (C1), 128.2 (C2''), 128.2 (C6''), 134.0 (C1''), 141.6 (C4'), 147.8 (C4), 148.1 (C3), 157.9 (C2'), 157.9 (C6'), 159.3 (C4''); HRMS (ESI) Calcd. for C<sub>23</sub>H<sub>25</sub>O<sub>5</sub> [M + H]<sup>+</sup> 381.1702, Found: 381.1703.

#### 4.1.14. [1,1':4',1''-Terphenyl]-2',3,4,4'',6'-pentaol (**3**)

Mp > 260 °C; <sup>1</sup>H NMR (600 MHz, DMSO-*d*<sub>6</sub>) δ 6.54 (s, 2H, H3', H5'), 6.58 (dd, *J* = 8.4, 1.8 Hz, 1H, H5), 6.69 (d, *J* = 8.4 Hz, 1H, H6), 6.73 (d, *J* = 1.8 Hz, 1H, H2), 6.83 (d, *J* = 8.4 Hz, 2H, H3'', H5''), 7.33 (d, *J* = 8.4 Hz, 2H, H2'', H6''), 8.69 (s, 2H, OH), 8.96 (s, 1H, OH), 9.52 (s, 1H, OH); <sup>13</sup>C NMR (600 MHz, DMSO-*d*<sub>6</sub>) δ 104.4 (C3'), 104.4 (C5'), 114.3 (C1'), 114.5 (C5), 115.5 (C3''), 115.5 (C5''), 118.5 (C2), 121.9 (C6), 125.3 (C1), 127.1 (C2''), 127.3 (C6''), 131.2 (C1''), 139.4 (C4'), 143.4 (C3), 143.9 (C4), 155.7 (C2'), 155.7 (C6'), 156.8 (C4''); HRMS (ESI) Calcd. for C<sub>18</sub>H<sub>15</sub>O<sub>5</sub> [M + H]<sup>+</sup> 311.0919, Found: 311.0907.

#### 4.1.15. [1,1'-Biphenyl]-4'-monol, 4-bromo-2,3-dimethoxy (**8b**)

Mp 117–118 °C; <sup>1</sup>H NMR (600 MHz, CDCl<sub>3</sub>) δ 3.65 (s, 3H, OCH<sub>3</sub>), 3.94 (s, 3H, OCH<sub>3</sub>), 5.57 (s, 1H, OH), 6.88 (d, *J* = 8.4 Hz, 2H, H3', H5'), 6.95 (d, *J* = 8.4 Hz, 1H, H5), 7.32 (d, *J* = 8.4 Hz, 1H, H6), 7.38 (s, *J* = 8.4 Hz, 2H, H2', H6'), <sup>13</sup>C NMR (600 MHz, CDCl<sub>3</sub>) δ 60.8 (OCH<sub>3</sub>), 60.9 (OCH<sub>3</sub>), 115.2 (C3'), 115.2 (C5'), 116.2 (C4), 126.4 (C6), 127.9 (C1), 129.7 (C5), 130.3 (C2'), 130.3 (C6'), 135.6 (C1'), 150.7 (C2), 151.5 (C3), 155.1 (C4'); HRMS (ESI) Calcd. for C<sub>14</sub>H<sub>13</sub>BrNaO<sub>3</sub> [M + Na]<sup>+</sup> 330.9946, Found: 330.9947.

#### 4.1.16. [1,1':4',1''-Terphenyl]-4''-monol,2',3',4'-tetramethoxy (**4a**)

Mp 165–166 °C; <sup>1</sup>H NMR (600 MHz, CDCl<sub>3</sub>) δ 3.69 (s, 3H, OCH<sub>3</sub>), 3.71 (s, 3H, OCH<sub>3</sub>), 3.93 (s, 3H, OCH<sub>3</sub>), 3.94 (s, 3H, OCH<sub>3</sub>), 5.09 (s, 1H, OH), 6.91 (d, *J* = 8.4 Hz, 2H, H3'', H5''), 6.96 (d, *J* = 8.4 Hz, 1H, H5), 7.12 (d, *J* = 7.8 Hz, 1H, H6'), 7.13 (d, *J* = 8.4 Hz, 1H, H6), 7.14 (d, *J* = 7.8 Hz, 1H, H5'), 7.18 (d, *J* = 1.8 Hz, 1H, H2), 7.47 (d, *J* = 8.4 Hz, 2H, H2'', H6''); <sup>13</sup>C NMR (600 MHz, CDCl<sub>3</sub>) δ 55.88 (OCH<sub>3</sub>), 55.9 (OCH<sub>3</sub>), 60.7 (OCH<sub>3</sub>), 60.8 (OCH<sub>3</sub>), 110.3 (C5), 110.9 (C2), 112.5 (C3''), 112.5 (C5''), 115.1 (C5'), 121.4 (C6'), 125.3 (C6), 125.4 (C1'), 130.4 (C2''), 130.4 (C6''), 130.5 (C4'), 130.8 (C1''), 134.8 (C1), 148.2 (C4), 148.5 (C3), 150.9 (C2'), 150.9 (C3'), 154.9 (C4''); HRMS (ESI) Calcd. for C<sub>22</sub>H<sub>23</sub>O<sub>5</sub> [M + H]<sup>+</sup> 367.1545, Found: 367.1547.

#### 4.1.17. [1,1':4',1''-Terphenyl]-2',3,3',4,4''-pentaol (**4**)

Mp > 260 °C; <sup>1</sup>H NMR (600 MHz, Methanol-*d*<sub>4</sub>) δ 6.80 (s, 2H, H3', H5'), 6.85 (d, *J* = 8.4 Hz, 1H, H5), 6.86 (d, *J* = 8.4 Hz, 2H, H3'', H5''), 6.94 (dd, *J* = 8.4, 1.8 Hz, 1H, H6), 7.09 (d, *J* = 1.8 Hz, 1H, H2), 7.45 (d, *J* = 8.4 Hz, 2H, H2'', H6''); <sup>13</sup>C NMR (600 MHz, Methanol-*d*<sub>4</sub>) δ 116.0 (C3''), 116.0 (C5''), 116.2 (C5), 117.4 (C2), 121.7 (C5'), 121.7 (C6'), 122.1 (C6''), 122.2 (C5'), 128.9 (C6), 129.1 (C1''), 131.2 (C2''), 131.3 (C6''),

131.7 (C1), 143.6 (C2'), 143.7 (C3'), 145.5 (C3), 146.0 (C4), 157.4 (C4''); HRMS (ESI) Calcd. for C<sub>18</sub>H<sub>15</sub>O<sub>5</sub> [M + H]<sup>+</sup> 311.0919, Found: 311.0913.

## 4.2. Biological assay

### 4.2.1. Cell line and reagents

MDA-MB-435 cell line was obtained from ATCC and cultured in DMEM/F12 with 10% heat-inactivated fetal bovine serum. Cultures were maintained in a humidified incubator at 37 °C in an atmosphere of 5% CO<sub>2</sub>. All the reagents used in this study, unless otherwise indicated, were purchased from Sigma (St. Louis, MO).

### 4.2.2. In vitro cytotoxicity assays

The cytotoxicity was measured by the MTT assay as described in the literature [36,37]. The cells plated in the wells of 96-well plates (Falcon, USA) were treated in triplicate with various concentrations of compounds for 72 h in 5% CO<sub>2</sub> incubator at 37 °C. After fresh medium being changed, a 20 μL aliquot of MTT solution (5 mg/mL) was added and incubated for 4 h at 37 °C. Then, 100 μL of triplex solution (10% SDS, 5% isobutanol, 12 mM HCl) was added to each well and incubated overnight at 37 °C. The absorbance of each well was determined by a microplate reader (M-3350, Bio-Rad) with a 590 nm wavelength. Growth inhibition rates were calculated with the following equation:

$$\text{Inhibition rate} = \frac{\text{OD control well} - \text{OD treated well}}{\text{OD control well} - \text{OD blank well}} \times 100\%$$

### 4.2.3. Cell cycle analysis

Cell cycle analysis was measured as previously described [38,39]. Briefly, 5 × 10<sup>5</sup> cells were plated in six-well plates. After drug treatment, the cells were fixed in 75% ethanol at –22 °C overnight, resuspended in 1 mL phosphate-buffered saline containing 0.1 mg/mL RNaseA and propidium iodide (40 μg/mL) to stain DNA for 30 min at room temperature, and analyzed for DNA contents using a FACScan flow cytometer (Beckman coulter EPICS<sup>XL</sup>). Data were analyzed using MultiCycle for windows software (Beckman coulter EPICS<sup>XL</sup>).

### 4.2.4. Analysis of apoptosis

**4.2.4.1. Nuclear staining with DAPI.** After treatment, cells were collected, washed once with 2 mL of ice-cold PBS, fixed with 1 mL 4% paraformaldehyde for 20 min, and then washed once again with 2 mL of ice-cold PBS. The cells were incubated in 1 mL of DAPI at 50 μg/mL containing 100 μg/mL RNaseA. This mixture was incubated for 30 min at 37 °C. After having been washed with 2 mL of PBS three times, the cells were observed using fluorescence microscopy at 340 nm (excitation) and 488 nm (emission).

### 4.2.4.2. Flow cytometric analysis (annexin V-FITC/PI staining) of phosphatidylserine exposure.

At the indicated times and doses of treatment, MDA-MB-435 cells were assayed for phosphatidylserine exposure, by using the Annexin V-FITC Apoptosis Detection Kit (Sigma) according to the manufacturer's instructions. Stained samples were analyzed by a FACScan flow cytometer (Beckman coulter EPICS<sup>XL</sup>). The fractions of cell population in different quadrants were analyzed using quadrant statistics. Cells in the lower right quadrant represented apoptosis while cells in the upper right quadrant represented necrosis or post apoptotic necrosis.

### 4.2.5. Western blot analysis

After treatment with or without compounds, cells were harvested and lysed in ice-cold lysis buffer (20 mM Tris-HCl, pH 7.4,

150 mM NaCl, 1 mM EDTA, 1 mM EGTA, 1% Triton, 2.5 mM sodium pyrophosphate, 1 mM  $\beta$ -glycerophosphate, 1 mM sodium orthovanadate, 1 mg/mL leupeptin, 1 mM phenylmethylsulfonyl fluoride). The lysates were clarified by centrifugation at 12,000 rpm at 4 °C for 15 min, mixed with an equal volume of 2 $\times$  loading buffer (4% SDS, 10% 2-mercaptoethanol, 20% glycerol, and 0.2 mg/mL bromophenol blue in 0.1 M Tris–HCl, pH 6.8), and then boiled for 10 min immediately. The boiled lysates were loaded onto 8–12% SDS-polyacrylamide gels and transferred to Immobilon-P membranes (Millipore). After blocked with 5% skim milk in phosphate-buffered saline with 0.1% Tween-20 for 1 h, the membranes were incubated with antibodies against  $\beta$ -actin, Bcl-2, Bak, Bad, caspase3, cleaved caspase-3, PARP, cyclin B1, cdc2, Myt1, GADD45 $\alpha$  and cdc25c (Cell Signaling Technology). Primary antibodies were detected using either peroxidase-conjugated ImmunoPure goat anti-rabbit IgG (H + L) or peroxidase-conjugated ImmunoPure Goat Anti-Mouse IgG (H + L) secondary antibody (Jackson ImmunoResearch, USA) and enhanced chemiluminescence.

#### 4.2.6. DNA gel electrophoresis assay of topoisomerases

Plasmid pBR322 DNA and purified calf thymus DNA topoisomerase I were purchased from TakaRa Biotechnology (Dalian) Co., Ltd., recombinant human topoisomerase II $\alpha$  was obtained from TopoGENINC (USA). All experiments were done at least in duplicate to confirm the results.

**4.2.6.1. DNA relaxation assay.** DNA topo I inhibition assay was performed as described previously [40] with minor modifications. The test compounds were dissolved in DMSO at 20 mM as stock solution. The activity of DNA Topo I was determined by assessing the relaxation of supercoiled DNA pBR322. The mixture of 0.5  $\mu$ g of plasmid pBR322 DNA and 1 units of Topo I was incubated without and with the prepared compounds at 37 °C for 30 min in the relaxation buffer (10 mM Tris–HCl (pH 7.9), 150 mM NaCl, 0.1% bovine serum albumin, 1 mM spermidine, 5% glycerol). The reaction in the final volume of 20  $\mu$ L was terminated by adding 2.5  $\mu$ L of the stop solution containing 5% sarcosyl, 0.0025% bromophenol blue, and 25% glycerol. DNA samples were then electrophoresed on a 1% agarose gel at 5 V/cm for 2 h with a running buffer of TAE. Gels were stained for 30 min in an aqueous solution of ethidium bromide (0.5  $\mu$ g/mL) and photographed under UV light.

DNA Topo II $\alpha$  inhibitory activity of compounds was measured as follows [41]. Briefly, the mixture of 0.5  $\mu$ g of supercoiled pBR322 plasmid DNA and 1 units of Topo II $\alpha$  was incubated without and with the prepared compounds in the assay buffer (10 mM Tris–HCl (pH 7.9) containing 50 mM NaCl, 50 mM KCl, 5 mM MgCl<sub>2</sub>, 1 mM EDTA, 1 mM ATP, and 15  $\mu$ g/mL bovine serum albumin) for 30 min at 30 °C. The reaction in a final volume of 20  $\mu$ L was terminated by the addition of 3  $\mu$ L of 7 mM EDTA. Reaction products were analyzed on a 1% agarose gel at 5 V/cm for 2 h with a running buffer of TAE. Gels were stained for 30 min in an aqueous solution of ethidium bromide (0.5  $\mu$ g/mL) and photographed under UV light.

**4.2.6.2. Cleavage assay of Topo I and Topo II $\alpha$ .** The enzymatic reactions were set in the same format as for the Topo I and Topo II $\alpha$  inhibition assays except that in the enzymatic reactions an increased amount of the enzyme (1 units per reaction) was used. These reaction mixtures were incubated at 37 °C for 30 min and immediately terminated with 2  $\mu$ L of 10% sodium dodecyl sulfate (SDS), followed by vigorous mixing. After the enzyme digestion with proteinase K (50  $\mu$ g/mL) for 20 min, gel loading buffer was added to the reaction mixture. Reaction mixture was analyzed on a 1% ethidium bromide-containing agarose gel at 5 V/cm for 2 h with a running buffer of TAE. Gels were destained in water and photographed under UV light.

**4.2.6.3. DNA-unwinding assay.** DNA-unwinding assay was employed to assess the ability of compound **1** of intercalating into plasmid DNA according to the procedure in previous studies [42]. Relaxed DNA was prepared by treatment of the supercoiled plasmid pBR322 with excess Topo I (10 units), followed by proteinase K digestion at 37 °C, phenol-chloroform extraction and ethanol precipitation. After incubation with testing compounds at 37 °C for 30 min, reactions were terminated by the addition of gel loading buffer and electrophoresed under the same conditions as described above. The DNA bands were stained with 0.5  $\mu$ g/mL of ethidium bromide and visualized by UV light.

**4.2.6.4. Topo II-mediated DNA decatenation assay.** Topo II activity was measured by the ATP-dependent decatenation of kDNA [43]. Briefly, 0.20  $\mu$ g of kDNA (TopoGEN, Inc) was incubated 2 unit of topoisomerase II $\alpha$  at 37 °C for 30 min in a total of 20  $\mu$ L reaction buffer [50 mM Tris (pH 8.0), 120 mM KCl, 10 mM MgCl<sub>2</sub>, 0.5 mM ATP, 0.5 mM DTT, 30  $\mu$ g/mL BSA]. The reaction was stopped with 2  $\mu$ L of 10% SDS. Samples were subjected to electrophoresis under the same conditions as described above.

#### Acknowledgments

This work was financially supported by NSFC Projects (81273384, 90913024).

#### Appendix A. Supplementary data

Supplementary data related to this article can be found at <http://dx.doi.org/10.1016/j.ejmech.2013.07.020>.

#### References

- [1] J.C. Wang, DNA topoisomerases, *Annu. Rev. Biochem.* 65 (1996) 635–692.
- [2] J.J. Champoux, DNA topoisomerases: structure, function, and mechanism, *Annu. Rev. Biochem.* 70 (2001) 369–413.
- [3] S. Salerno, F. Da Settimo, S. Taliani, F. Simorini, C. La Motta, G. Fornaciari, A.M. Marini, Recent advances in the development of dual topoisomerase I and II inhibitors as anticancer drugs, *Curr. Med. Chem.* 17 (2010) 4270–4290.
- [4] W.A. Denny, Dual topoisomerase I/II poisons as anticancer drugs, *Expert Opin. Invest. Drugs* 6 (1997) 1845–1851.
- [5] K. Chikamori, A.G. Grozav, T. Kozuki, D. Grabowski, R. Ganapathi, M.K. Ganapathi, DNA topoisomerase II enzymes as molecular targets for cancer chemotherapy, *Curr. Cancer Drug Targets* 10 (2010) 758–771.
- [6] V. Call, C. Spatafora, C. Tringali, Polyhydroxy-p-terphenyls and related p-terphenylquinones from fungi: overview and biological properties, in: R. Atta ur (Ed.), *Studies in Natural Products Chemistry*, Elsevier, 2003, pp. 263–307.
- [7] T. Kamiguchi, R. Sakazaki, K. Nagashima, Y. Kawamura, Y. Yasuda, K. Matsushima, H. Tani, Y. Takahashi, K. Ishii, R. Suzuki, K. Koizumi, H. Nakai, Y. Ikenishi, Y. Terui, Terpenins, novel immunosuppressants produced by *Aspergillus candidus*, *J. Antibiot. (Tokyo)* 51 (1998) 445–450.
- [8] S.S. Liu, B.B. Zhao, C.H. Lu, J.J. Huang, Y.M. Shen, Two new p-terphenyl derivatives from the marine fungal strain *Aspergillus* sp. AF119, *Nat. Prod. Commun.* 7 (2012) 1057–1062.
- [9] A. Barzilai, K. Yamamoto, DNA damage responses to oxidative stress, *DNA Repair (Amst)* 3 (2004) 1109–1115.
- [10] G. Iliakis, Y. Wang, J. Guan, H. Wang, DNA damage checkpoint control in cells exposed to ionizing radiation, *Oncogene* 22 (2003) 5834–5847.
- [11] V.A. Rao, C. Conti, J. Guirouilh-Barbat, A. Nakamura, Z.H. Miao, S.L. Davies, B. Sacca, I.D. Hickson, A. Bensimon, Y. Pommier, Endogenous gamma-H2AX-ATM-Chk2 checkpoint activation in Bloom's syndrome helicase deficient cells is related to DNA replication arrested forks, *Mol. Cancer Res.* 5 (2007) 713–724.
- [12] Y. Tsujimoto, Bcl-2 family of proteins: life-or-death switch in mitochondria, *Biosci. Rep.* 22 (2002) 47–58.
- [13] A.K. Larsen, A.E. Escargueil, A. Skladanowski, Catalytic topoisomerase II inhibitors in cancer therapy, *Pharmacol. Ther.* 99 (2003) 167–181.
- [14] J.M. Fortune, N. Osheroff, Topoisomerase II as a target for anticancer drugs: when enzymes stop being nice, *Prog. Nucleic Acid Res. Mol. Biol.* 64 (2000) 221–253.
- [15] W. Shi, S.L. Marcus, T.L. Lowary, Cytotoxicity and topoisomerase I/II inhibition of glycosylated 2-phenyl-indoles, 2-phenyl-benzo[b]thiophenes and 2-phenyl-benzo[b]furans, *Bioorg. Med. Chem.* 19 (2011) 603–612.
- [16] Y. Pommier, J. Covey, D. Kerrigan, W. Mattes, J. Markovits, K.W. Kohn, Role of DNA intercalation in the inhibition of purified mouse leukemia (L1210) DNA

- topoisomerase II by 9-aminoacridines, *Biochem. Pharmacol.* 36 (1987) 3477–3486.
- [17] A.R. Chowdhury, S. Sharma, S. Mandal, A. Goswami, S. Mukhopadhyay, H.K. Majumder, Luteolin, an emerging anti-cancer flavonoid, poisons eukaryotic DNA topoisomerase I, *Biochem. J.* 366 (2002) 653–661.
- [18] H.L. Gomez, J.A. Pinto, M. Olivera, T. Vidaurre, F.D. Doimi, C.E. Vigil, R.G. Velarde, J.E. Abugattas, E. Alarcon, C.S. Vallejos, Topoisomerase II- $\alpha$  as a predictive factor of response to therapy with anthracyclines in locally advanced breast cancer, *Breast* 20 (2011) 39–45.
- [19] K. Kawachi, T. Sasaki, A. Murakami, T. Ishikawa, A. Kito, I. Ota, D. Shimizu, A. Nozawa, Y. Nagashima, R. Machinami, I. Aoki, The topoisomerase II  $\alpha$  gene status in primary breast cancer is a predictive marker of the response to anthracycline-based neoadjuvant chemotherapy, *Pathol. Res. Pract.* 206 (2010) 156–162.
- [20] R. van Gijn, R. Lendfers, J. Schellens, A. Bult, J. Beijnen, Dual topoisomerase I/II inhibitors, *J. Oncol. Pharm. Pract.* 6 (2000) 92–108.
- [21] A.M. Azarova, Y.L. Lyu, C.P. Lin, Y.C. Tsai, J.Y. Lau, J.C. Wang, L.F. Liu, Roles of DNA topoisomerase II isozymes in chemotherapy and secondary malignancies, *Proc. Natl. Acad. Sci. U. S. A.* 104 (2007) 11014–11019.
- [22] K. Luo, Z. Lou, Dual roles of topoisomerase II, *Cell Cycle* 8 (2009) 679.
- [23] D.J. Clarke, A.C. Vas, C.A. Andrews, L.A. Diaz-Martinez, J.F. Gimenez-Abian, Topoisomerase II checkpoints: universal mechanisms that regulate mitosis, *Cell Cycle* 5 (2006) 1925–1928.
- [24] G.K. Schwartz, M.A. Shah, Targeting the cell cycle: a new approach to cancer therapy, *J. Clin. Oncol.* 23 (2005) 9408–9421.
- [25] L.A. Diaz-Martinez, D.J. Clarke, Chromosome cohesion and the spindle checkpoint, *Cell Cycle* 8 (2009) 2733–2740.
- [26] N. Fujikawa, T. Ohta, T. Yamaguchi, T. Fukuda, F. Ishibashi, M. Iwao, Total synthesis of lamellarins D, L, and N, *Tetrahedron* 62 (2006) 594–604.
- [27] K. Nishizawa, J.Y. Satoh, The reaction of cycloalkanones with copper(II) halides. II. The reaction of cyclohexanones with copper(II) bromide, *Bull. Chem. Soc. Jpn.* 48 (1975) 1875–1877.
- [28] K. Nishizawa, J.Y. Satoh, A convenient synthesis of substituted pyrocatechols, *Bull. Chem. Soc. Jpn.* 48 (1975) 2215–2216.
- [29] M. Albrecht, Synthesis of linear oligo(catechol) ligands for the metal directed self-assembly of helicates, *Synthesis* 2 (1996) 230–236.
- [30] M.E.L. Jung, Patrick Yuk Sun, Mansuri, M. Muzzamil, Speltz, M. Laurine, Stereoselective synthesis of an analog of podophyllotoxin by an intramolecular Diels–Alder reaction, *J. Org. Chem.* 50 (1985) 1087–1105.
- [31] A.L.K. Jarugu Narasimha Moorthy, Subhas Samanta, Ankur Roy, Werner M. Nau<sup>[b]</sup>, Modulation of spectrokinetic properties of o-quinonoid reactive intermediates by electronic factors: time-resolved laser flash and steady-state photolysis investigations of photochromic 6- and 7-Arylchromenes, *Chem. Eur. J.* 15 (2009) 4289–4300.
- [32] J.S.F.H.E. Landis, An expeditious aqueous Suzuki–Miyaura methodology for the arylation of bromophenols, *Tetrahedron Lett.* 47 (2006) 4275–4279.
- [33] S.M.N. Widyastuti, Fukuji, Keisuke Watanabe, Nobumichi Sako, Kinji Tanaka, Isolation and characterization of two aucuparin-related phytoalexins from *Photinia glabra Maxim.*, *Ann. Phytopathol. Soc. Jpn.* 58 (1992) 228–233.
- [34] M. Roberti, D. Pizzirani, M. Recanatini, D. Simoni, S. Grimaudo, A. Di Cristina, V. Abbadessa, N. Gebbia, M. Tolomeo, Identification of a terphenyl derivative that blocks the cell cycle in the G0–G1 phase and induces differentiation in leukemia cells, *J. Med. Chem.* 49 (2006) 3012–3018.
- [35] D.E. Frantz, D.G. Weaver, J.P. Carey, M.H. Kress, U.H. Dolling, Practical synthesis of aryl triflates under aqueous conditions, *Org. Lett.* 4 (2002) 4717–4718.
- [36] J. Carmichael, W.G. DeGraff, A.F. Gazdar, J.D. Minna, J.B. Mitchell, Evaluation of a tetrazolium-based semiautomated colorimetric assay: assessment of chemosensitivity testing, *Cancer Res.* 47 (1987) 936–942.
- [37] Y. Huang, J. Wang, G. Li, Z. Zheng, W. Su, Antitumor and antifungal activities in endophytic fungi isolated from pharmaceutical plants *Taxus mairei*, *Cephalotaxus fortunei* and *Torreya grandis*, *FEMS Immunol. Med. Microbiol.* 31 (2001) 163–167.
- [38] T. Ohtsuki, T. Koyano, T. Kowithayakorn, N. Yamaguchi, M. Ishibashi, Isolation of austroinulin possessing cell cycle inhibition activity from *Blumea glomerata* and revision of its absolute configuration, *Planta Med.* 70 (2004) 1170–1173.
- [39] J. Wang, B. Zhao, W. Zhang, X. Wu, R. Wang, Y. Huang, D. Chen, K. Park, B.C. Weimer, Y. Shen, Mycoepoxydiene, a fungal polyketide, induces cell cycle arrest at the G2/M phase and apoptosis in HeLa cells, *Bioorg. Med. Chem. Lett.* 20 (2010) 7054–7058.
- [40] M. Fukuda, K. Nishio, F. Kanzawa, H. Ogasawara, T. Ishida, H. Arioka, K. Bojanowski, M. Oka, N. Saijo, Synergism between cisplatin and topoisomerase I inhibitors, NB-506 and SN-38, in human small cell lung cancer cells, *Cancer Res.* 56 (1996) 789–793.
- [41] J.F. Barrett, J.A. Sutcliffe, T.D. Gootz, In vitro assays used to measure the activity of topoisomerases, *Antimicrob. Agents Chemother.* 34 (1990) 1–7.
- [42] Y. Yamashita, N. Fujii, C. Murakata, T. Ashizawa, M. Okabe, H. Nakano, Induction of mammalian DNA topoisomerase I mediated DNA cleavage by antitumor indolocarbazole derivatives, *Biochemistry* 31 (1992) 12069–12075.
- [43] L. Du, H.C. Liu, W. Fu, D.H. Li, Q.M. Pan, T.J. Zhu, M.Y. Geng, Q.Q. Gu, Unprecedented citrinin trimer tricitinol B functions as a novel topoisomerase II $\alpha$  inhibitor, *J. Med. Chem.* 54 (2011) 5796–5810.